Spin and charge fluctuation in an extended Hubbard model of oxide superconductors

Aniket Bhattacharya* and C. S. Wang
Department of Physics and Center for Superconductivity Research, University of Maryland, College Park, Maryland 20742
(Received 16 April 1993)

Antiferromagnetic spin fluctuations and charge-transfer correlation are studied in an extended Hubbard model of cuprate superconductors. We have carried out finite-temperature Monte Carlo and variational Monte Carlo simulations of CuO_2 lattices described by a three-band Hubbard model. Using parameters derived by local-density-functional theory, our results appear to be consistent with experimental data. At half-filling, we find strong antiferromagnetic correlation with large local moment on copper sites and evidence of a charge-transfer gap. Upon doping, the antiferromagnetic correlations decrease; the excess holes primarily go onto the oxygen sites, while additional electrons prefer the copper sites. Equal-time pairing correlation functions suggest that extended *s*-wave and *d*-wave pairing are possible in this model.

I. INTRODUCTION

A common feature of all high-T_c oxide superconductors is the existence of CuO_2 layers. The intermediate layers existing between any two such planes serve as charge reservoirs for doping, also stabilize the long-range order of the superconducting phase. It was proposed that the electrons, in the two-dimensional CuO_2 planes are highly correlated and quantum fluctuations beyond the mean-field approximation are important. The electron-electron correlation can be described by the extended three-band Hubbard model on a square CuO_2 lattice, which is often approximated, either by a one-band Hubbard model, or in the large-U limit by the one-band t-J model.[1] Many theories of electronic origin have been proposed as the pairing mechanism for superconductivity. In particular, the RVB theory[1] proposed by Anderson and co-workers, the spin-bag theory of Schrieffer, Wen, and Zhang,[2] and the anyonic theory of Laughlin,[3] are all based on single-band model. The single-band model is valid when the on-site energy difference between the Cu-*d* and O-*p* bands is large compared to the bandwidth. It is a Mott insulator at half-filling. Away from half-filled limit, however, photoemission experiments have suggested that holes are predominantly oxygen in character, which raise some doubts about the validity of the one-band models. On the theoretical side, Varma, Schmitt-Rink, and Abrahams[4] have identified the insulating material as a charge-transfer insulator. They proposed a mechanism for superconductivity with attractive pairing interaction arising from charge-transfer excitations, e.g., $Cu^{2+}O^{2-} \rightarrow Cu^{1+}O^{1-}$, where the energy is lowered by the interband Coulomb repulsion. This theory does not require the presence of large-U terms, rather it needs low density of the carrier and near degeneracy of the oxygen-*p* and copper-*d* levels. Another mechanism which requires a multiband extended Hubbard model is due to Emery.[5] In this theory, superconductivity in the doped system is due to presence of oxygen holes. Hybridization between the copper and the oxygen orbitals gives rise to a strong antiferromagnetic (AFM) exchange interaction between them, which destroys the Cu-Cu AFM correlation. The extra *p* holes may form superconducting pairs mediated by the magnetic interactions.

These theoretical models of superconductivity are all plausible solutions to the extended Hubbard model in different parameter spaces. Numerical simulations guided by the experimental data serve to determine the physically relevant parameter space for the cuprate superconductors. The extended Hubbard model has been studied quite extensively using various methods, e.g., quantum Monte Carlo methods,[6] variational Monte Carlo simulation,[7] exact diagonalization of small clusters,[8] and various perturbative schemes. The complexity of the model renders examination of the phase diagram difficult. The effects of the intersite Coulomb repulsion are of particular interest, because several calculations using exact diagonalization of small clusters[9] and slave-boson technique[10] seem to indicate that the intersite Coulomb term may be responsible for the origin of electron pairing. Furthermore, Lin, Hirsh, and Scalapino,[11] have shown that a single-U Hubbard model, which is responsible for antiferromagnetism, cannot account for superconductivity.

In this paper we present results for the three-band Hubbard model on a square CuO_2 lattice, using (1) finite-temperature quantum Monte Carlo (FTQMC) simulations, and (2) variational quantum Monte Carlo simulations (VQMC) with Gutzwiller wave functions.[12] For smaller CuO_2 lattices, we found excellent agreement between these two methods. The efficiency of the VQMC method has enabled us to study up to 6×6 lattices. Results are presented for spin- and charge-correlation functions. It is anticipated that experimental observations will put severe constraints on the parameters of this model Hamiltonian.

Although there have been several quantum Monte Carlo calculations on the multiband Hubbard model, our work compliments earlier calculations by including a more complete and/or more realistic parameter regime. For example some of the earlier calculations chose a phase factor such that all the hopping parameters have

0163-1829/93/48(18)/13949(10)/$06.00

the same sign. In this work, on the contrary, the parameters for the extended Hubbard model are chosen as estimated by either a supercell or cluster geometry calculations within the local-density approximation.[13–15] Our calculations indicate that the appropriate choice of these parameters is important in order to study high-temperature superconductivity. Otherwise, similar calculations but with different parameters may result in, as we have shown in one particular case, qualitatively different conclusions. Recently, VQMC simulations were reported by Coppersmith,[7] where (1) the oxygen-oxygen hopping was taken to be zero, and (2) the staggered magnetic field, that generates the variational antiferromagnetic wave functions, was kept a small but fixed value. Near half-filling, we found stronger antiferromagnetic correlations, but most of our conclusions are qualitatively consistent with Coppersmith's calculations.

II. THE EXTENDED HUBBARD MODEL

Near E_F, the most important feature of the band structure[16] of all high-T_c copper oxides is the antibonding $pd\sigma$ band, which is exactly half-filled in stoichiometric La_2CuO_4. This $pd\sigma$ band can be viewed as the mean-field solution of the following extended Hubbard-Anderson model:

$$H = t_{pd}\sum_{i,l,\sigma}[d^{\dagger}_{i,\sigma}p_{l,\sigma}+\text{H.c.}] + t_{pp}\sum_{l,m,\sigma}[p^{\dagger}_{l,\sigma}p_{m,\sigma}+\text{H.c.}]+U_d\sum_{i,\sigma}n_{d,i\uparrow}n_{d,i\downarrow} + U_p\sum_{l,\sigma}n_{p,l\uparrow}n_{p,l\downarrow}+U_{pd}\sum_{i,l\sigma}n_i n_l+\epsilon\sum_l n_{p,l}\ , \quad (1)$$

where i, l, and m run over copper and oxygen sites, respectively; the set of points $l \in i$ are positions of four oxygen sites surrounding the copper site at i, and the set of points $m \in l$ are positions of two nearest-neighbor oxygen to the oxygen site at l; σ denotes the spins. The $d^{\dagger}(d)$ and $p^{\dagger}(p)$ create (destroy) a hole on the copper $3d_{x^2-y^2}$ and O_{2p} sites. The parameters U_d, U_p, and U_{pd} are the on-site Coulomb repulsion on the copper and oxygen sites, and the intersite Coulomb repulsion between nearest-neighbor copper and oxygen sites, respectively: ϵ is the bare on-site energy difference between copper and oxygen sites. The parameters t_{pd}, t_{pp} are the amplitudes for a hole to hop from an oxygen site to an adjacent copper site and oxygen site, respectively. The Slater-Koster parameters $t_{pd}=\pm(\sqrt{3}/2)V_{pd\sigma}$ hybridizes the nearest-neighbor Cu_{3d} and O_{2p} orbitals and $t_{pp}=\pm\sqrt{1}/2(V_{pp\sigma}-V_{pp\pi})$ allows direct O_{2p}-O_{2p} hopping. The $\pm$ signs are according to the Salter-Koster table for two centered integrals.[17] Note that many of the existing theoretical calculations have chosen phase factors such that all the t_{pp}'s and all the t_{pd}'s have the same hopping sign. Our calculations suggest that such an approximation may result in different qualitative conclusions.

Much of the theoretical efforts have been devoted to estimate the appropriate parameters using either supercell[13,14] or cluster geometry,[15] within the local-density approximation (LDA). The Coulomb repulsions are calculated from the total energy either as a function of the occupation of Cu_{3d} and O_{2p} orbitals, or based on the transition-state approximation. The resulting parameters are in the range $U_d=5-12$ eV, $U_p=4-14$ eV, and $U_{pd}=0.6-2$ eV. The rest of the parameters can be obtained from the tight-binding fit to first-principle energy bands. However, the limitation of the LDA to stabilize the AFM ground state in La_2CuO_4 is well established, and the uncertainties in certain parameters (ϵ in particular) may be quite large. According to the classification of Zannen, Zwatsky, and Allen[18] for an Anderson impurity, $U_{pd}=0.6-2$ eV may fall into the category of charge-transfer insulator with large fluctuations in the metallic phase.

III. METHODS

Different numerical techniques may provide valuable insights to the physics of strongly correlated electron systems in absence of exact solutions. The method of exact diagonalization tends to be limited by finite-size effects, while FTQMC strictly applied to finite temperature. For ground-state properties, the VQMC method is numerically more stable and more practical for larger systems. A direct comparison of the results of the FTQMC and VQMC for smaller lattices or simplified model Hamiltonians, would shed some light on the question of (1) the role of finite temperature, (2) the validity of the variational wave functions, and (3) finite-size effects. Unless otherwise specified, results presented here are based on VQMC simulations of up to 6×6 lattices.

A. Finite-temperature Monte Carlo simulations

For FTQMC simulations we used the computer simulation programs developed previously by McQueen and Wang[19] for quantum simulation of the Anderson lattice Hamiltonian, where the algorithm of Blankenbecler, Scalapino, and Sugar[20] for fermionic Monte Carlo simulation is used in a manner similar to Hirsch's simulation on the Hubbard model.[21] In this approach the discrete Hubbard-Stratonovich transformation[22] is used to replace the two-fermion interaction with that of a free electron interacting with a time-dependent Ising field, and the Metropolis method is used to carry out the sum over the Ising spins. The intersite Coulomb repulsion between nearest-neighbor copper-oxygen atoms are incorporated exactly, by introducing additional Ising spins between neighboring copper and oxygen sites. In order to achieve stability at low temperature, we also implemented the modified-Grams-Schmidt decomposition scheme introduced by Loh and Gubernatis.[23]

B. Variational Monte Carlo simulations

For VQMC we used a stochastic algorithm developed by McQueen and Wang,[24] which maps the Gutzwiller matrix elements onto a statistical model that can be evaluated in a manner similar to FTQMC scheme. This approach has been applied successfully to study the Anderson model,[19] and more recently to study the role of generalized flux phases in a single-band Hubbard model.[25]

The trial wave function is a generalization of the Gutzwiller wave function:

$$|\psi\rangle = \prod_{i,j} [(1-g_d)n_{d,i\uparrow}n_{d,i\downarrow}][(1-g_p)n_{p,j\uparrow}n_{p,j\downarrow}]|\psi_0\rangle \ , \tag{2}$$

where g_d and g_p are variational parameters that govern the fractional double occupancy at the copper and oxygen sites, respectively. $|\psi_0\rangle$ is the eigenstate of a renormalized tight-binding Hamiltonian H_0. In the mean-field limit, the effect of the U_{pd} term is to renormalize the bare on-site energy difference between the copper and the oxygen levels. Thus, the on-site energy difference ε_0 in H_0 should be treated as a variational parameter to optimize the trial wave functions. However, within the range of U_{pd} of interest, we find our results are not sensitive to ε_0 so that we set $\varepsilon_0=\epsilon$. Finally, to describe the electron-spin correlation, we use the following spin-density wave states:

$$|\psi_{\rm AFM}\rangle = \exp[h(n_{d,i\uparrow}-n_{d,i\downarrow})]|\psi_0\rangle \ . \tag{3}$$

There are four variational parameters, g_d, g_p, ε_0, and h, which are optimized to minimize the energy. Among them, g_d is the most sensitive parameter, which can be seen from Fig. 1. In Fig. 1(a), $\langle n_d \rangle$ and $\langle n_p \rangle$ are shown as a function of g_d, while the corresponding $\langle n_{d\uparrow}n_{d\downarrow} \rangle$, and $\langle n_d n_p \rangle$ are shown in Figs. 1(b) and 1(c), respectively. Near half-filling, increasing g_d will enhance the probability of double occupancy at the copper sites, which moves charges from the oxygen to the copper sites. Accordingly, $\langle n_{d\uparrow}n_{d\downarrow} \rangle$ increases with increasing g_d. However, the nearest-neighbor Coulomb repulsion decreases because

$$\langle (n_d+\delta)(n_p-\delta) \rangle = \langle n_d n_p \rangle - \delta(\langle n_d \rangle + \langle n_p \rangle) + \delta^2 \ . \tag{4}$$

The kinetic energy is *lowered* because holes become more mobile when the probability of double occupancy is raised. The effect of g_p is similar to that of g_d, but less prominent because the oxygen levels are sparsely populated. With an on-site energy difference about 2–3 eV, nearly 70% of the holes are on the copper sites and the oxygen sites are barely doubly occupied. Thus we keep $g_p=1.0$ in most cases.

IV. RESULTS

As a first approximation, we set $U_p=0$ and $t_{pp}=0$ in order to compare the results from FTQMC with that of VQMC on a 4×4 square lattice. This is a reasonable starting point, because there is not too much intra-atomic Coulomb repulsion on the oxygen sites, when most of the holes are concentrated at the copper sites. For this simplified model, the tight-binding part of the Hamiltonian produces the following dispersion relation, for the bonding and the antibonding bands:[16]

$$E(k_x,k_y) = \frac{(\epsilon_p+\epsilon_d)}{2} \pm \frac{(\epsilon_p-\epsilon_d)^2}{2} + 4t_{pd}\left[\sin\left[\frac{kx}{2}\right]^2 + \sin\left[\frac{ky}{2}\right]^2\right] . \tag{5}$$

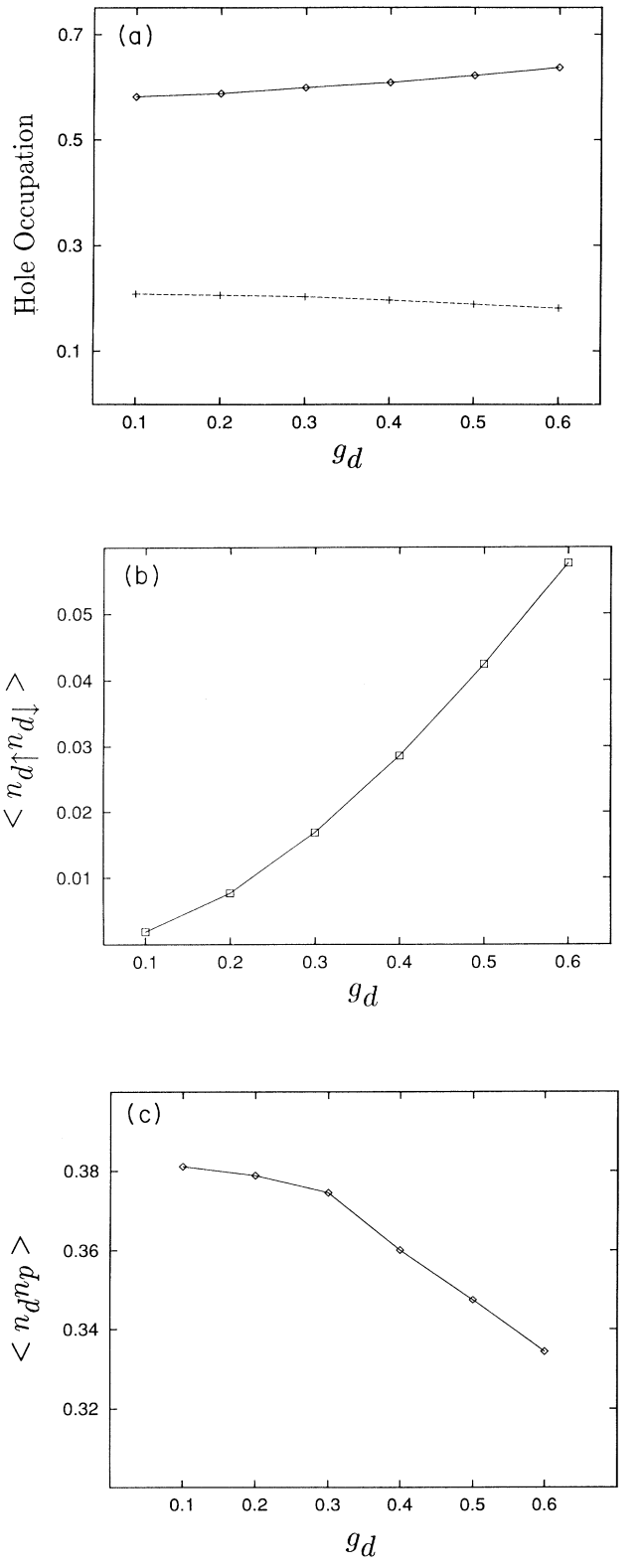

FIG. 1. Dependence of (a) $\langle n_d \rangle$, $\langle n_p \rangle$, (b) $\langle n_{d\uparrow}n_{d\downarrow} \rangle$, (c) $\langle n_d n_p \rangle$ on g_d. In (a), the diamond and the plus signs represent the copper and the oxygen atoms, respectively. Lines drawn through the points are a guide to the eye.

We note that the bandwidth of either band is

$$W=\sqrt{(\epsilon/2)^2+8}-\epsilon/2\ . \tag{6}$$

When $U_d>\epsilon>2$ the charge-transfer energy exceeds the bandwidth W, but less than the Coulomb energy U_d. The system is then characterized by a charge-transfer gap.[18] If $\epsilon>U_d$, however, the oxygen levels are so far away that one can integrate out completely,[26] and the system becomes a Mott insulator at half-filling.

A. Dependence on n for $U_d=6$, $U_p=0$, $U_{pd}=0$, $\epsilon=2$, and $t_{pp}=0$

Figure 2(a) shows the VQMC simulation of $\langle n_d\rangle$ and $\langle n_p\rangle$ as a function of the hole filling factor, $n=\langle n_p+2n_d\rangle$. Clearly, these parameters are in the charge-transfer regime because the extra holes beyond half-filling primarily go to the oxygen sites, while additional electrons mostly go to the copper sites. These results are in excellent agreement with that obtained from our FTQMC simulations shown in Fig. 2(b).

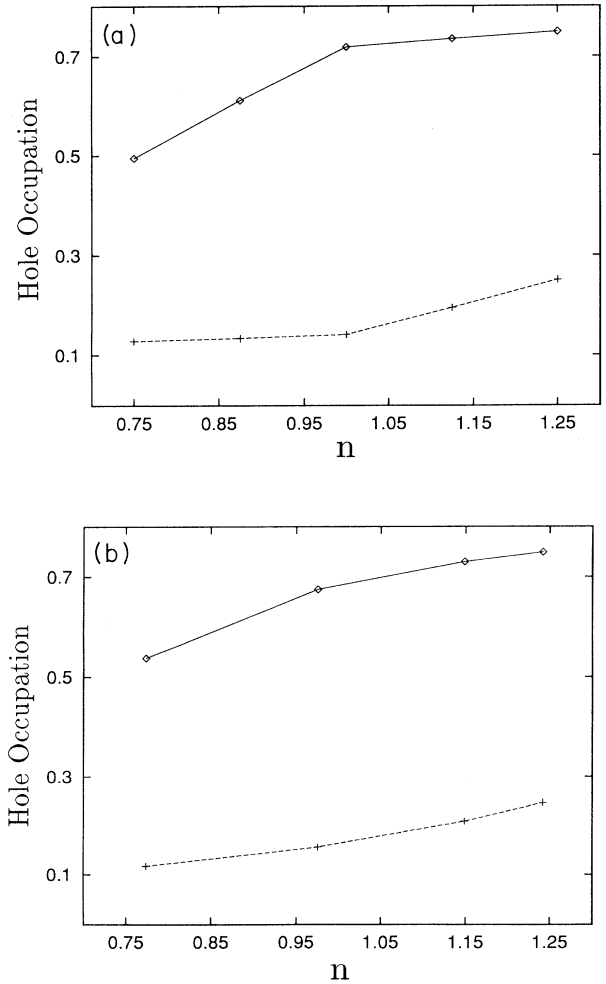

FIG. 2. (a) VQMC and (b) FTQMC simulations of copper and oxygen hole occupation as a function of doping $n=\langle n_d+2n_p\rangle$ on a 4×4 lattice for $U_d=6.0$ and $\epsilon=2.0$ at half-filling. The temperature for FTQMC was $0.156\,25t_{pd}$. Lines drawn through the points are a guide to the eye.

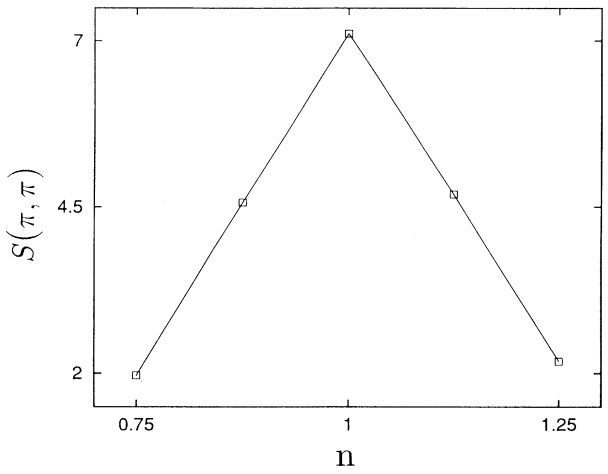

FIG. 3. Magnetic structure factor $S(\pi,\pi)$ as a function of doping $n=\langle n_d+2n_p\rangle$ on a 4×4 lattice for $U_d=6.0$ and $\epsilon=2.0$. Lines drawn through the points are a guide to the eye.

Our results, derived from the VQMC and the FTQMC simulations are compared in Table I. At half-filling, the system is antiferromagnetic. Accordingly, the results of our calculations using AFM trial wave functions are very close to that of finite-temperature simulations. Figure 3 shows the density dependence of magnetic structure factor $S(\pi,\pi)$, derived from VQMC, for $U_d=6$ and $\epsilon=2$. Away from half-filling, the AFM correlation is significantly suppressed.

B. Dependence on ϵ for $U_d=6$, $U_p=0$, $U_{pd}=0$, $\epsilon=2$, and $t_{pp}=0$

At half-filling, the variation of (a) $\langle n_d\rangle$ and $\langle n_p\rangle$, (b) $\langle n_{d\uparrow}n_{d\downarrow}\rangle$, and (c) the copper-site local moment, are shown, as a function of ϵ, in Fig. 4. As ϵ increases, holes move from the oxygen to the copper sites. The local moment at the copper site increases to avoid on-site Coulomb repulsion U_d, and $\langle n_{d\uparrow}n_{d\downarrow}\rangle$ decreases gradually. This can also be understood from the second-order perturbation theory. The effective bandwidth for the copper-copper hopping is given by $t_{\rm eff}=t^2/\epsilon$. As ϵ increases, the ratio $U_d/t_{\rm eff}$ increases. Therefore, $\langle n_{d\uparrow}n_{d\downarrow}\rangle$

TABLE I. Comparison of FTQMC and VQMC results for a 4×4 lattice for $U_d=6.0$ and $\epsilon=2.0$ at half-filling. The temperature for FTQMC was $0.156\,25t_{pd}$.

	FTQMC	VQMC
$\langle n_d\rangle$	0.691±0.003	0.691±0.003
$\langle n_p\rangle$	0.312±0.003	0.309±0.003
$\langle$KE$\rangle$	−1.960±0.01	−1.978±0.01
$\langle n_{d\uparrow}n_{d\downarrow}\rangle$	0.009±0.0001	0.010±0.0001
$\langle n_dn_p\rangle$	0.239±0.005	0.251±0.005
$\langle\mu_d\rangle$	0.674±0.005	0.634±0.005

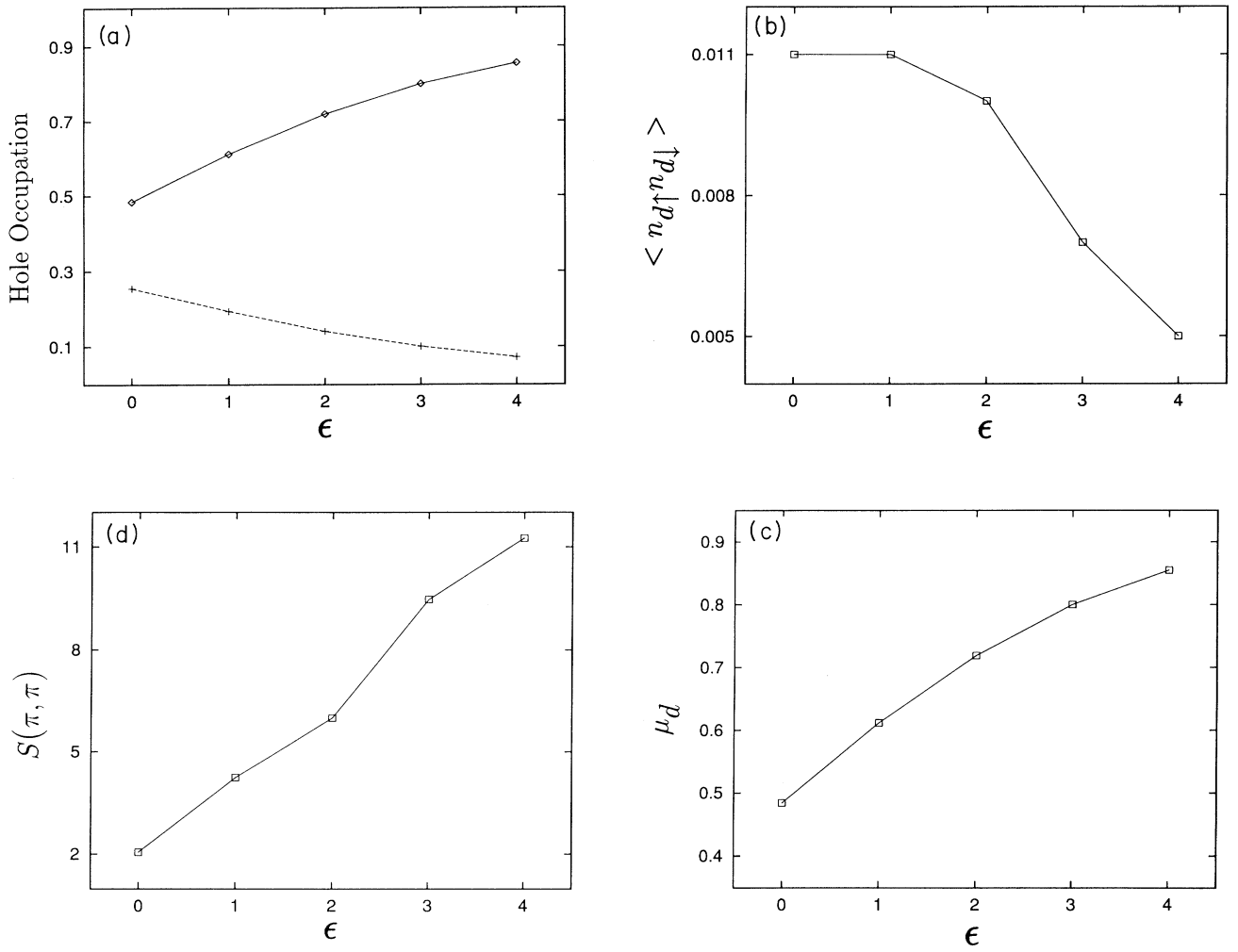

FIG. 4. (a) site occupancies $\langle n_d \rangle$ and $\langle n_p \rangle$, (b) double occupancies $\langle n_{d\uparrow} n_{d\downarrow} \rangle$, (c) moment $\langle \mu_d \rangle$, and magnetic structure factor $S(\pi,\pi)$ as a function of on-site energy difference ϵ for $U_d = 6.0$ on a 4×4 lattice. The symbols in (a) have the same meaning as in Fig. 1(a). Lines drawn through the points are a guide to the eye.

is suppressed, while the magnetic moment, given by

$$\mu_d = (n_{d,i\uparrow} - n_{d,i\downarrow})^2 = n_{d\uparrow}^2 + n_{d\downarrow}^2 - 2n_{d\uparrow} n_{d\downarrow} \quad (7)$$

increases monotonically as a function ϵ.

As can be seen from Fig. 4(d), the AFM structure factor increases monotonically with increasing ϵ. Antiferromagnetism promotes hopping so that holes are delocalized. As ϵ increases, there is a cancellation of energies between kinetic energy and copper-site Coulomb repulsion. These results are consistent with the results of Scallettar *et al.*,[6] although they have chosen the hopping phases to be uniform.

C. Dependence on t_{pp} for $U_d = 10$, $U_p = 0$, $U_{pd} = 1$, $n = 1$, and $\epsilon = 2$

The role of t_{pp} is of particular interest, because the earlier calculations of Li and Callaway[8] for a small Cu_2O_4 cluster exhibited a drastic phase separation, with holes either localized on the oxygen sites or on the copper sites near $t_{pp} \sim 0.8 t_{pd}$. We consider identical parameters employed by Li and Callaway: $U_d = 10$, $U_d = 10$, $U_p = 0$, $U_{pd} = 1$, and $\epsilon = 2$, with uniformly negative $t_{pd} = -1.0$, and keeping all the t_{pp} values uniformly positive. For a 2×2 lattice, the results of our VQMC calculations are in good agreement with the results of Li and Callaway for exact diagonalization. The copper and the oxygen hole occupations are shown in Fig. 5(a) as a function of t_{pp}. There is a clear phase separation for $t_{pp} \leq 0.85$. However, the phase separation is exaggerated by the finite-size effects, which is evident from the results for a 4×4 lattice show in Fig. 5(b). Moreover the phase separation disappears when appropriate signs for t_{pd} and t_{pp} are taken into account: The results for 2×2 lattice are shown in Fig. 5(c), while results for the 4×4 lattice are shown in Fig. 5(d).

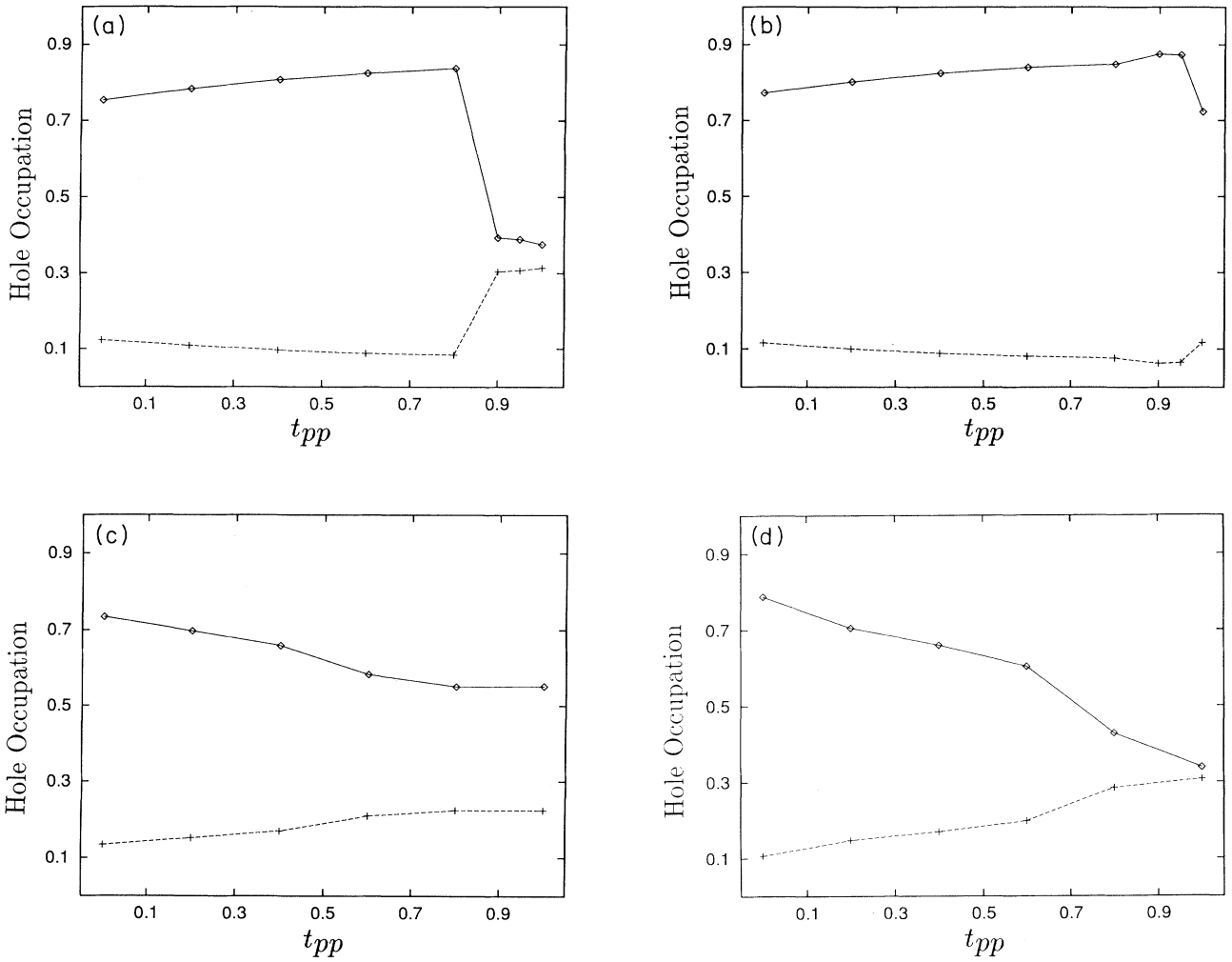

FIG. 5. Copper and oxygen hole occupation $\langle n_d \rangle$ and $\langle n_p \rangle$, as a function of t_{pp}, at half-filling for $U_d = 10.0$, $U_{pd} = 1.0$. The results for all t_{pd} negative, and all t_{pp} positive, are shown for 2×2 (a), and for 4×4 lattices (b). For appropriate hopping signs for cuprate superconductors, the corresponding results are shown in (c) and (d), respectively. The symbols have the same meaning as in Fig. 1(a). Lines drawn through the points are a guide to the eye.

D. Dependence on U_{pd}

We now study the effect of the nearest-neighbor interaction between copper and oxygen sites. For $n = 1.0$, $U_d = 6$, and $\epsilon = 2$, we study the effect of U_{pd} on a 4×4 lattice in Fig. 6. As shown in Fig. 6(a), $\langle n_p n_d \rangle$ decreases as U_{pd} increases, to minimize the interatomic Coulomb repulsion. This can also be understood in the Hartree-Fock approximation, where the effects of U_{pd} are to renormalize the bare on-site energy:

$$\bar{\epsilon}_d = \epsilon_d + \frac{U_d \langle n_d \rangle}{2} + 4U_{pd}\langle n_p \rangle \ ,$$
$$\bar{\epsilon}_p = \epsilon_p + \frac{U_p \langle n_d \rangle}{2} + 2U_{pd}\langle n_p \rangle \ . \tag{8}$$

As already shown in Fig. 2, holes move from the oxygen to copper sites and $\langle n_p n_d \rangle$ decreases, when the effective $\epsilon = \epsilon_p - \epsilon_d$ increases. Other than the charge transfer, $\langle n_d \rangle$ and $\langle n_p \rangle$ shown in Fig. 6(b) ($U_d = 10$, $U_{pd} = 1.0$, and $\epsilon = 2.0$) exhibit similar dependence on hole concentration as in Fig. 2(a) ($U_d = 6$, $U_{pd} = 1.0$, and $\epsilon = 2.0$). The system remains a charge-transfer insulator.

E. The LDA parameters: $U_d = 8$, $U_p = 3$, $U_{pd} = 1.0$, and $t_{pp} = 0.5$

We now consider the three-band Hubbard model using parameters predicted by local-density-functional theory. The most sensitive and uncertain parameter is the on-site energy difference. At half-filling, $\langle n_d \rangle$ and $\langle n_p \rangle$ are shown in Fig. 7(a) as a function of ϵ, for $U_d = 8.0$, $U_p = 3.0$, $U_{pd} = 0.9$, and $t_{pp} = 0.5$. An on-site energy difference of $\sim 2-3$ eV will produce the correct site occupancies and local moment: roughly 65–75 % holes on copper sites with a local moment of ~ 0.70. The occu-

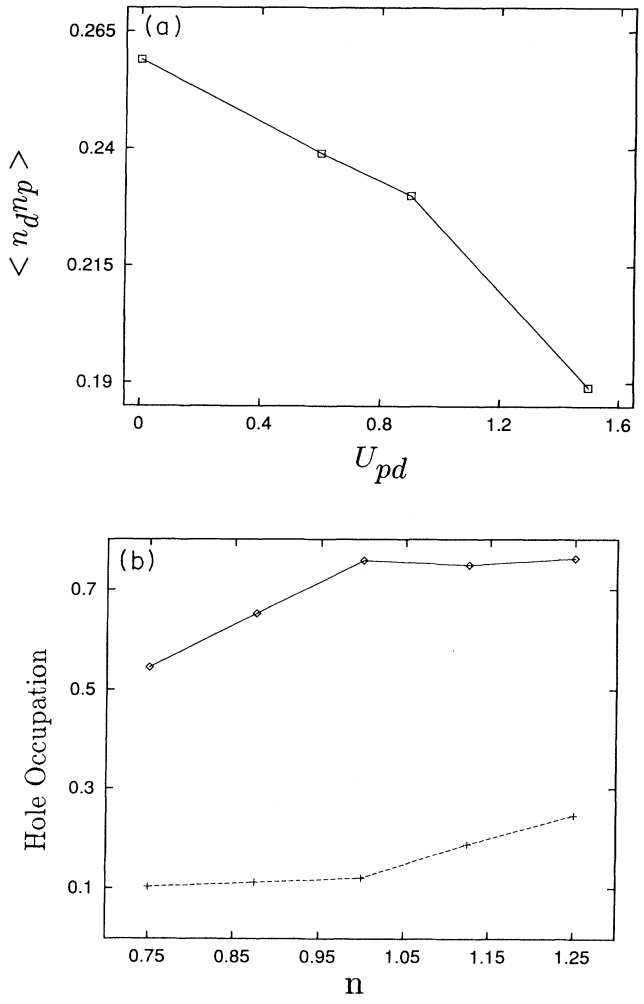

FIG. 6. Dependence of (a) $\langle n_p n_d \rangle$, and (b) copper and oxygen hole occupation on U_{pd} for $U_d = 10.0$, and $\epsilon = 2.0$ for a 4×4 lattice. The symbols in (b) have the same meaning as in Fig. 1(a). Lines drawn through the points are a guide to the eye.

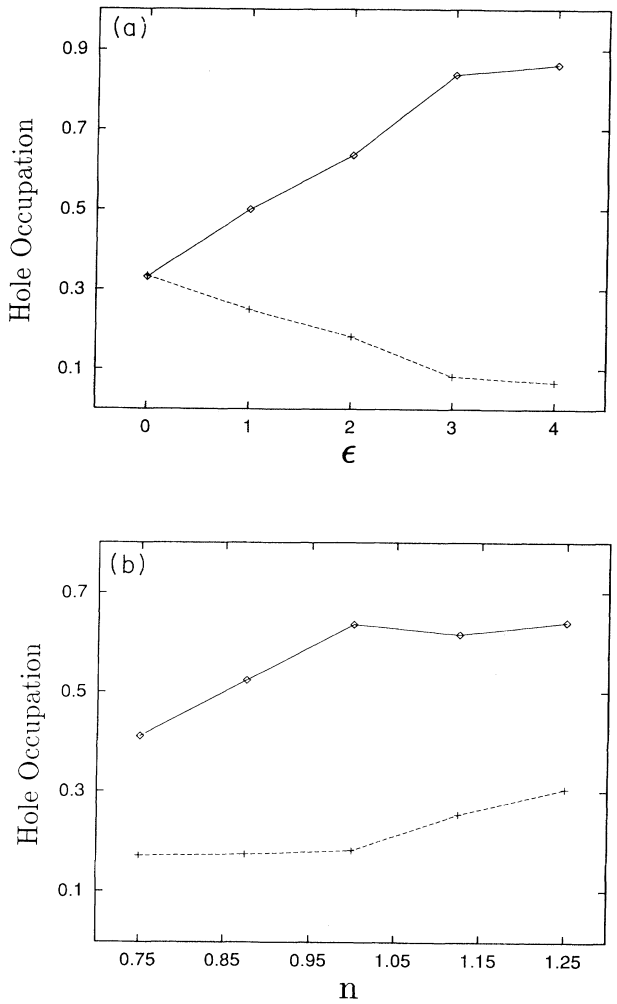

FIG. 7. Dependence of copper and oxygen hole occupation $\langle n_d \rangle$ and $\langle n_p \rangle$ on (a) ϵ at half-filling, and on $\langle n = n_d + 2n_p \rangle$ for $U_d = 8.0$, $U_p = 3.0$, $U_{pd} = 0.9$, $t_{pp} = 0.5$, and $\epsilon = 2.8$. Appropriate hopping signs for cuprate superconductors are taken into account. The symbols have the same meaning as in Fig. 1(a). Lines drawn through the points are a guide to the eye.

pancies are shown in Fig. 7(b) as a function of $n = \langle n_p + 2n_d \rangle$. Similar calculations have been reported by Coppersmith[7] using a different VQMC scheme. In Coppersmith's calculation, the staggered magnetic field h that generates the AFM wave function [see Eq. (3)] was kept at small but a fixed value. We found qualitatively bigger differences in energies between paramagnetic and antiferromagnetic states, specially at and near half-filling. But qualitatively our results are consistent with Coppersmith's calculations.

For the same set of parameters, we have performed FTQMC on four unit cells. In Tables II and III we have compared our results for FTQMC with VQMC results for four unit cells, both at half-filling, and at a hole density of 1.25 per site. It is evident that the agreement is good. In FTQMC all the interaction terms are treated exactly, including the nearest-neighbor Coulomb interaction. In VQMC, this term was treated in the mean-field approximation. At exact half-filling we get almost the same value of $\langle n_p n_d \rangle$ from both sets of calculations. Away from half-filling, the value of $\langle n_p n_d \rangle$ from FTQMC is $\sim 10\%$ less than what we get from VQMC. Nonetheless the agreement is reassuring.

TABLE II. Comparison of FTQMC and VQMC results for a 2×2 lattice for $U_d = 8.0$, $U_p = 3.0$, $U_{pd} = 0.9$, $\epsilon = 2.8$, and $t_{pp} = 0.5$ at half-filling. The temperature for FTQMC was $0.045 t_{pd}$.

	FTQMC	VQMC
$\langle n_d \rangle$	0.679±0.005	0.691±0.003
$\langle n_p \rangle$	0.321±0.005	0.309±0.003
$\langle n_d n_p \rangle$	0.236±0.003	0.240±0.003
$\langle$KE$\rangle$	−2.5±0.01	−2.39±0.01
$\langle n_{d\uparrow} n_{d\downarrow} \rangle$	0.009±0.0001	0.010±0.0001
$\langle \mu_d \rangle$	0.659±0.005	0.684±0.005
Energy	−1.35±0.05	−1.24±0.01

TABLE III. Comparison of FTQMC and VQMC results for a 2×2 lattice for $U_d=8.0$, $U_p=3.0$, $U_{pd}=0.9$, $\epsilon=2.8$, and $t_{pp}=0.5$ at $\langle n\rangle=1.25$. The temperature for FTQMC was $0.045t_{pd}$.

	FTQMC	VQMC
$\langle n_d\rangle$	0.784±0.005	0.750±0.003
$\langle n_p\rangle$	0.466±0.005	0.500±0.003
$\langle n_d n_p\rangle$	0.517±0.003	0.578±0.003
⟨KE⟩	−2.93±0.05	−3.07±0.01
$\langle n_{d\uparrow} n_{d\downarrow}\rangle$	0.034±0.0001	0.044±0.0001
$\langle \mu_d\rangle$	0.717±0.005	0.662±0.005
Energy	−0.85±0.05	−0.72±0.01

F. Finite-size effects of magnetic structure factors

To show how the physical quantities scale with lattice size, our VQMC results for 2×2, 4×4, and 6×6 lattices are compared in Table IV. At half-filling, the system exhibits an AFM peak in the magnetic structure factor. Away from half-filling it is less prominent. The scaled magnetic structure factor at half-filling is shown in Fig. 8 as a function of lattice size, while the temperature dependence is shown in Fig. 9.

G. Superconducting correlation functions

Electron pairing from purely electronic origin has been discussed for both the single and multiband Hubbard models.[27] In a finite-size system, true off-diagonal long-range order cannot be studied because the particle number is not conserved. In addition, the lowest temperature attainable in FTQMC is close to magnetic ordering, while superconductivity occurs at a much lower energy. Since the temperature scale of the effective interaction is expected to be higher than T_c, it may be possible to determine if the effective interaction is attractive. In particular, pairing susceptibilities can be calculated in the particle-particle channel. In the case of a one-band Hubbard model White *et al.*[28] pointed out that the pair susceptibility may be misleading. To study the sign of the effective interaction, it is important to subtract out the uncorrelated susceptibility.

In FTQMC simulation, two-particle interactions are replaced by space and imaginary-time-dependent Hubbard-Stratonovich field. The interactions are calculated by Monte Carlo sampling over these fields. If the averaging on the single-particle Green's function is performed *before* taking their products, then the effects of the interaction are removed, and one gets the corresponding *uncorrelated susceptibilities.* By subtracting out this uncorrelated part from the actual susceptibilities, one can study the effects of the interaction. White *et al.*[28] introduced this method and studied the particle-hole and particle-particle pairing susceptibilities in the single-band Hubbard model. Near half-filling, they found $d_{x^2-y^2}$ susceptibility most attractive.

We have studied the static particle-particle susceptibilities in the multiband extended Hubbard model. Similar calculation was done by Li and Callaway[8] using the exact

TABLE IV. Comparison of VQMC results for 2×2, 4×4, and 6×6 lattices for $U_d=8.0$, $U_p=3.0$, $U_{pd}=0.9$, $\epsilon=2.8$, and $t_{pp}=0.5$ at half-filling.

	2×2	4×4	6×6
$\langle n_d\rangle$	0.705±0.003	0.717±0.003	0.719±0.001
$\langle n_p\rangle$	0.295±0.003	0.282±0.003	0.281±0.001
$\langle n_d n_p\rangle$	0.240±0.003	0.230±0.001	0.230±0.0007
⟨KE⟩	−2.39±0.01	−2.239±0.005	−2.251±0.002
$\langle n_{d\uparrow} n_{d\downarrow}\rangle$	0.010±0.0001	0.0061±0.0005	0.0085±0.0004
$\langle \mu_d\rangle$	0.684±0.005	0.705±0.004	0.702±0.004
Energy	−1.24±0.01	−1.163±0.005	−1.163±0.005

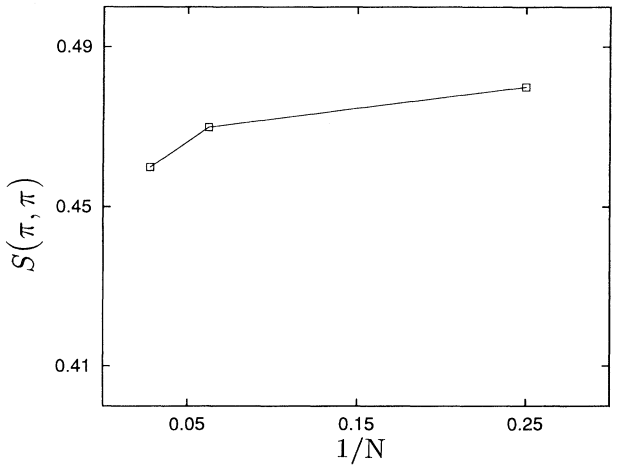

FIG. 8. Size dependence of magnetic structure factor $S(\pi,\pi)$ at half-filling for 2×2, 4×4, and 6×6 lattices ($U_d=8.0$, $U_p=3.0$, $U_{pd}=0.9$, $t_{pp}=0.5$, and $\epsilon=2.8$). Lines drawn through the points are a guide to the eye.

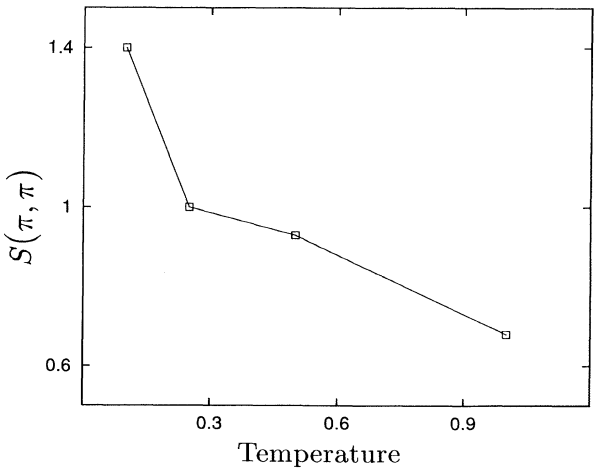

FIG. 9. Magnetic structure factor $S(\pi,\pi)$ as a function of temperature for $U_d=8.0$, $U_p=3.0$, $U_{pd}=0.9$, $t_{pp}=0.5$, and $\epsilon=2.8$ on a 2×2 lattice. Lines drawn through the points are a guide to the eye.

diagonalization method. We consider the following cases.

Local singlet:

$$\Delta_s = \Delta_0 \ . \tag{9}$$

Extended s wave:

$$\Delta_s = (\Delta_x + \Delta_{-x} + \Delta_y + \Delta_y) \ . \tag{10}$$

d wave:

$$\Delta_d = (\Delta_x + \Delta_{-x} - \Delta_y - \Delta_y) \ , \tag{11}$$

where Δ is given by

$$\Delta = \sum_{\mathbf{a}} d_{\mathbf{r}+\mathbf{a}\uparrow} d_{\mathbf{r}\downarrow} \ . \tag{12}$$

The sum over **a** should be different for different symmetries. The equal-time pair correlation is given by

$$P = \langle \Delta \Delta^\dagger \rangle \ . \tag{13}$$

Subtracting the single-particle contribution, the pairing interaction is given by

$$\langle d_{\mathbf{r}+\mathbf{a}\uparrow} d_{\mathbf{r}\downarrow} \rangle \langle d^\dagger_{\mathbf{s}\downarrow} d^\dagger_{\mathbf{s}+\mathbf{a}\uparrow} \rangle - \langle d_{\mathbf{r}+\mathbf{a}\uparrow} d^\dagger_{\mathbf{s}+\mathbf{a}\uparrow} \rangle \langle d_{\mathbf{r}\downarrow} d^\dagger_{\mathbf{s}\downarrow} \rangle \ . \tag{14}$$

Here the operator $d_s^\dagger$ creates a hole on either copper or oxygen sites.

The first of the above expression is evaluated using Wick's theorem. The second part is the product of average Green's functions $G_\uparrow(\mathbf{r}+\mathbf{a},\mathbf{s}+\mathbf{a})$ and $G_\downarrow(\mathbf{r},\mathbf{s})$. In Fig. 10, we have plotted the extended-*s* and *d*-wave pairing as a function of temperature. Both of them become increasingly positive at lower temperature indicating the possibility of pairing in the extended Hubbard model. Our results are consistent with similar calculations of Sclattar *et al.*[6] and a recent random-phase approximation calculation.[29]

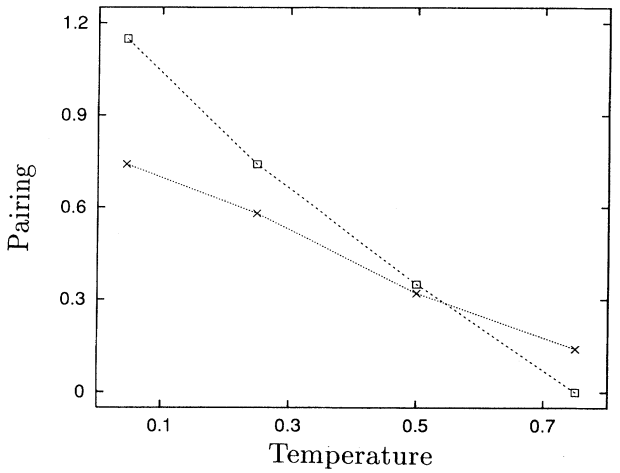

FIG. 10. Variation of *d*-wave (crosses) and extended-*s* wave (plus signs) pairing as a function of temperature for $U_d = 8.0$, $U_p = 3.0$, $U_{pd} = 0.9$, $t_{pp} = 0.5$, and $\epsilon = 2.8$ on a 2×2 lattice. Lines drawn through the points are a guide to the eye.

V. CONCLUSION

In summary we have tried to identify the parameter regime of an extended Hubbard model of oxide superconductors, within experimental constraints. For parameters consistent with the LDA, we find the ground to be antiferromagnetic with local moment of about 0.70. The single-particle features, e.g., site occupation, local moment, etc. are also consistent with a simplified model, in which U_p and U_{pd} are set to zero. From our FTQMC calculations, we note that a mixture of the extended-*s* and *d*-wave pairing is possible. But in absence of a proper finite-size scaling, it is not possible to settle this issue.

ACKNOWLEDGMENTS

The authors would like to thank P. G. McQueen for numerous discussion at the initial stage of this project. This work was supported in part by NSF (Grant No. DMR-8901453) with additional support from the Center for Superconductivity Research. The computer calculations were carried out under the auspices of Pittsburgh Supercomputing Center and at the University of Maryland.

*Present address: Department of Chemistry, The Pennsylvania State University, 152 Davey Laboratory, University Park, PA 16802.

[1]P. W. Anderson, Science **235**, 1196 (1987); G. Baskaran, Z. Zou, and P. W. Anderson, Solid State Commun. **63**, 973 (1987).

[2]J. R. Schrieffer, X.-G. Wen, and S. C. Zhang, Phys. Rev. Lett. **60**, 944 (1988); Phys. Rev. B **39**, 11 663 (1989).

[3]R. B. Laughlin, Science **242**, 525 (1988).

[4]C. M. Varma, S. Schmitt-Rink, and E. Abrahams, Solid State Commun. **62**, 681 (1987).

[5]V. J. Emery, Phys. Rev. Lett. **58**, 2794 (1988).

[6]R. T. Scalettar, D. J. Scalapino, R. L. Sugar, and S. R. White, Phys. Rev. B **44**, 770 (1991).

[7]S. N. Coppersmith, Phys. Rev. B **41**, 8771 (1990).

[8]Qiming Li and Joseph Callaway (unpublished).

[9]J. E. Hirsch, S. Tang, E. Loh, and D. J. Scalapino, Phys. Rev. Lett. **60**, 1668 (1989).

[10]C. A. Balseiro, M. Avignon, A. G. Rojo, and B. Alascio, Phys. Rev. Lett. **62**, 2624 (1989).

[11]H. Q. Lin, J. E. Hirsch, and D. J. Scalapino, Phys. Rev. B **37**, 7359 (1988).

[12]M. C. Gutzwiller, Phys. Rev. Lett. **10**, 159 (1963), Phys. Rev. **6A**, 159 (1963).

[13]M. Hybersten, M. Schlutter, and N. E. Christensen, Phys. Rev. B **39**, 9028 (1989).

[14]A. K. McMahan, R. M. Martin, and S. Sathpathy, Phys. Rev. B **38**, 6650 (1988).

[15]A. Fujimori, E. Takayama-Muromachi, Y. Uchida, and B. Okai, Phys. Rev. B **35**, 8814 (1987); Zhi-xun Shen, J. W. Al-

len, J. J. Yeh, J. S. Kang, W. Willis, W. Spicer, I. Lindau, M. B. Maple, Y. D. Dalichauch, M. S. Torikachvili, J. Z. Sun, and T. H. Geballe, *ibid.* **36**, 8414 (1987).
[16]L.F. Mattheiss, Phys. Rev. B **58**, 1028 (1987).
[17]J. C. Slater and G. F. Koster, Phys. Rev. **94**, 1498 (1954).
[18]J. Zaanen, G. S. Zwatszky, and J. W. Allen, Phys. Rev. Lett. **55**, 418 (1985).
[19]P. G. McQueen and C. S. Wang, Phys. Rev. B **44**, 10021 (1991).
[20]R. Blankenbecler, D. J. Scalapino, and R. L. Sugar, Phys. Rev. D **24**, 2278 (1981).
[21]J. E. Hirsch, Phys. Rev. B **31**, 4403 (1985); also look at S. R. White, D. J. Scalapino, R. L. Sugar, E. Y. Loh, J. E. Gubernatis, and R. T. Scalettar, *ibid.* **40**, 506 (1989), *for more recent studies.*
[22]J. E. Hirsch, Phys. Rev. B **28**, 4059 (1983).
[23]Eugene Loh and J. E. Gubernatis, in *Electronic Phase Transitions,* edited by W. Hanke and Y. V. Kopaev (North-Holland Elsevier, New York, 1990).
[24]P. G. McQueen and C. S. Wang, Phys. Rev. B **39**, 12414 (1989).
[25]Aniket Bhattacharya and C. S. Wang, Phys. Rev. B **45**, 10826 (1992).
[26]F. C. Zhang and T. M. Rice, Phys. Rev. B **37**, 3759 (1988).
[27]N. E. Bickers, D. J. Scalapino, and S. R. White, Phys. Rev. B **62**, 961 (1988).
[28]S. R. White, D. J. Scalapino, R. L. Sugar, and N. E. Bickers, Phys. Rev. B **39**, 839 (1989).
[29]P. B. Littlewood, C. M. Varma, S. Schmidt-Rink, and E. Abrahams, Phys. Rev. B **39**, 12371 (1989); R. Putz, B. Ehlers, L. Lilly, A. Muramatsu, and W. Hanke, *ibid.* **41**, 853 (1990).